Complexation of Diserinol Isophthalamide with Phosphorylated Biomolecules in Electrospray Ionization Mass Spectrometry

Madeline Schultz, Neil A. Ellis, Nwanne D. Banor, and Daniel A. Thomas*

Department of Chemistry, University of Rhode Island, Kingston, RI 02881

*To whom correspondence should be addressed: dathomas@uri.edu, (401) 874-5834, 140 Flagg Rd., Kingston, RI 02881

Graphical Abstract

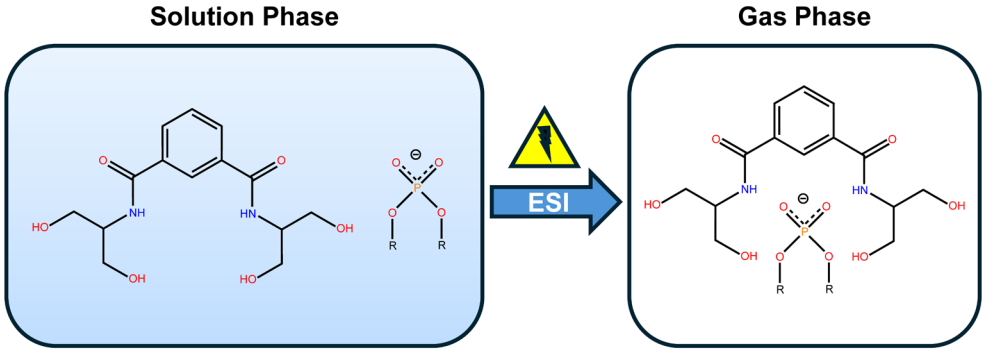

Abstract

Electrospray ionization (ESI) enables gentle transfer of biomolecules from solution to vacuum, facilitating the study of biomolecular structure under highly controlled conditions. However, biomolecules are desolvated during the ESI process, and the loss of ionic hydrogen bonds to solvent molecules can drive structural rearrangement, most prominently at solvent-exposed charge sites. Microsolvation reagents can bind to these bare charge sites in ESI mass spectrometry (ESI–MS) experiments, providing alternative intermolecular interaction partners. Previously, 18-crown-6 was shown to be an effective reagent for binding to cationic monoalkylammonium residues. More recently, diserinol isophthalamide (DIP) was reported as an analogous anionic microsolvation reagent, primarily for carboxylate residues of small model peptides. Herein, we expand upon this work to examine the complexation of DIP, 1,1'-(1,2-phenylene)bis(3-phenylurea) (PBP), and triclocarban (TCC) with molecules featuring a terminal or linking phosphate moiety. Specifically, using ESI–MS, we assess the binding of these reagents with dimethyl phosphate (DMP), cyclic adenosine monophosphate (cAMP), dibutyryl cAMP, RNA dinucleotides ApU and CpG, and angiotensin II phosphate (DRVpYIHPF). For DMP, the smallest target molecule, reagents TCC, PBP and DIP showed favorable adduction. However, for larger systems, PBP and TCC showed reduced complexation, which was attributed to steric hindrance from the terminal aromatic moieties of PBP and the limited hydrogen bonding network of TCC. Overall, of the three reagents, DIP showed the most consistent performance for anionic microsolvation of phosphate groups, facilitating future studies of gas-phase biomolecular structure and the effects of microsolvation.

1. Introduction

When biomolecules are brought from solution to the vacuum of a mass spectrometer (MS) via electrospray ionization (ESI), their local environment changes as solvent-biomolecule interactions, specifically hydrogen bonding networks, are lost.[1-5] The loss of intermolecular interactions can drive structural change,[6] with new low-energy conformers stabilized by intramolecular hydrogen bonding. These structural changes often occur via side-chain collapse at charged moieties previously stabilized by ionic hydrogen bonds with solvent.[6-10]

Microsolvation reagents can form noncovalent complexes with solvent-accessible charge sites during the electrospray process, thereby providing alternative intermolecular interactions.[11] This approach has been demonstrated through the complexation of 18-crown-6 (18C6) and other crown ethers to cationic monoalkylammonium moieties, specifically at lysine residues and the N-terminus.[11-21] The adduction process has also been shown to preferentially increase the signal of complexed species, which is attributed to enhanced surface activity during ESI that arises from the decrease in free energy of solvation upon complexation formation.[11] The effect of this complexation depends on the nature of the biomolecule studied and the experimental conditions. For biomolecules that lack a well-defined solution structure (typically smaller systems) or under conditions that impart significant energy to the biomolecular ions within the mass spectrometer, the complexation of 18C6 alters the potential energy landscape in vacuum, disfavoring conformations that feature intramolecular hydrogen bonds to reagent binding sites.[14] In this context, microsolvation reagents provide a useful tool for assessing the contribution of inter- vs intramolecular interactions to the observed molecular structure.[10, 14, 19, 20, 22]

Scheme 1. Reagents for Anion Microsolvation

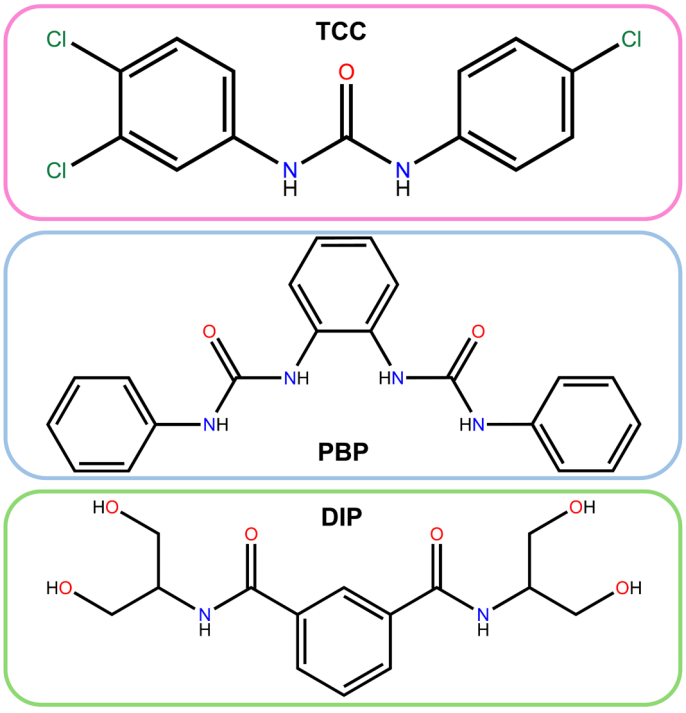

For systems with well-defined structure in solution, typically proteins, complexation with 18C6 has facilitated the study of three-dimensional structure under vacuum conditions. Specifically, ion mobility spectrometry (IMS) and ultraviolet photodissociation (UVPD) in combination with MS have shown that the complexation of 18C6 to peptides and proteins can reduce structural rearrangement and therefore preserve a native-like conformation in vacuum.[8, 9, 23] This preservation of secondary and tertiary structure

is accomplished through the formation of an intermolecular hydrogen bonding network between 18C6 and cationic moieties, disfavoring rearrangement driven by intramolecular solvation between the cationic moiety and the backbone or side chains . Additionally, selective non-covalent adduct protein probing (SNAPP) has been used as a probe of solution-phase structure by taking advantage of preferred adduction of 18C6 at solvent-accessible cationic moieties.[13, 18, 24]

Whereas 18C6 and other crown ethers have been extensively studied for complexation of cationic groups, there has been minimal work regarding complexation of anionic moieties, such as carboxylates and phosphates, for structural retention and microsolvation studies by ESI-MS. We previously reported the use of a novel reagent, diserinol isophthalamide (DIP), as well as a commercially available reagent, 1,1′-(1,2-phenylene)bis(3-phenylurea) (PBP),[25] for complexation with biomolecular anions during ESI–MS. Complexation was observed at the carboxylate groups of small peptides and at the phosphate and/or carboxylate groups of phosphorylated amino acids.[26] Herein, we expand upon this work to further examine binding of microsolvation reagents to phosphate moieties of biomolecules, specifically nucleic acids and phosphorylated peptides. Additionally, another commercially available antimicrobial agent, 3-(4-chlorophenyl)-1-(3,4-dichlorophenyl)urea, commonly referred to as triclocarban (TCC), is examined.[27] DIP, PBP and TCC (Scheme 1) were selected because of their comparatively small size, sterically accessible binding site, and propensity to complex via an extended hydrogen bonding network.[26, 28-30]

2. Methods and Materials

2.1 Collection of Mass Spectra

Tributyl(methyl) phosphonium dimethyl phosphate was purchased from Synthonix (Wake Forest, NC). Cytosine-guanine RNA dinucleotide (CpG) and adenine-uracil RNA dinucleotide (ApU) were purchased from TriLink Biotechnologies (San Diego, CA). 1,1'-(1,2-phenylene)bis(3-phenylurea) (PBP), triclocarban (TCC), adenosine 3',5'-cyclic monophosphate sodium salt monohydrate (cAMP), and N^6,2'-O-dibutyryladenosine 3',5'-cyclic monophosphate sodium salt (DBcAMP) were purchased from Sigma-Aldrich (St. Louis, MO). Angiotensin II phosphate (DRVpYIHPF) was purchased from InnoPep (San Diego, CA). All reagents were used as supplied. Diserinol isophthalamide (DIP) was synthesized as described previously.[26] To prepare 1 mM solutions, CpG, ApU, DIP, and DMP were dissolved in H_2O; TCC was dissolved in MeOH, and PBP was dissolved in 90/10 MeOH/ DMSO (v/v %). From the prepared 1 mM stocks, all samples were prepared in 80/20 H_2O/MeOH (v/v%) with concentrations of 10 μM analyte and 30 μM complexation reagent, except for angiotensin II phosphate, where a complexation reagent concentration of 90 μM was used. Mass spectra were collected in negative mode on a Shimadzu 2020 instrument in 80/20 (v/v%) H_2O/MeOH at a flow rate of 20 μL/min. An injection volume of 10 μL was used. All spectra were collected in triplicate.

2.2 Electronic Structure Calculations

Conformational searching for complexes between DMP and DIP, PBP, or TCC was performed using the conformer-rotamer ensemble sampling tool (CREST) developed by Pracht, Grimme, and co-workers.[31-33] The semi-empirical tight binding method, GFN2,[34] was used with the default energy window of 6 kcal mol^{-1}. Structural optimization of these complexes was then performed using the ORCA 5.0.3 software package.[35, 36] The hybrid density functional B3LYP[37-39] was used with the Grimme empirical dispersion correction and Becke-Johnson damping (D3BJ).[40, 41] The def2-TZVP basis set was used for all calculations.[42] For B3LYP calculations, the RIJCosX approximation[43] was used with auxiliary basis set def2/J.[44] The lowest-energy conformers identified for each of the three complexation agents were also optimized using Møller-Plesset second order perturbation (MP2) with the resolution of identity approximation[45, 46] and auxiliary basis sets def2-TZVP/C[47] and def2/J.[44, 48]

3. Results and Discussion

Complexation of microsolvation reagents to a variety of molecules containing either terminal or central phosphate moieties was investigated. To account for the varying ionization efficiencies of the phosphate species and the microsolvation reagents studied,[49] complexation is quantified by a ratio of the intensity of the bound complex to the unbound free phosphate anion, bound:unbound. The intensities used in the bound:unbound ratios were taken as the sum of intensities for all detected isotopes.

Scheme 2. Phosphate-Containing Molecules Studied

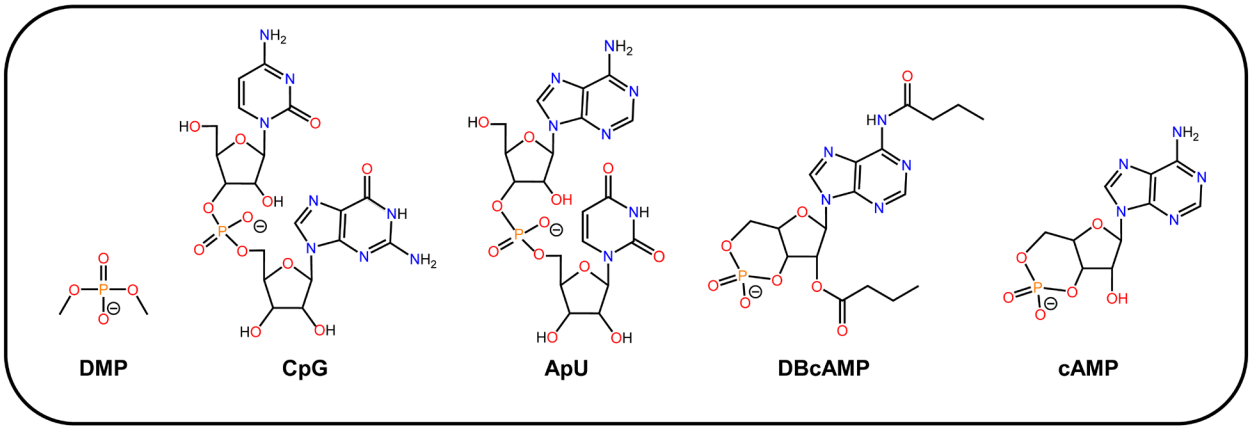

3.1 DMP Complexation

To examine reagent complexation propensity with minimal steric effects, we began by studying adduction to dimethyl phosphate (DMP, Scheme 2), for which large flanking moieties are absent. As seen in Figure 1, significant adduction to dimethyl phosphate was observed for all microsolvation reagents studied. For both PBP and DIP (Figures 1B and 1C, respectively), only a 1:1 complex between reagent and anionic DMP was observed. In contrast, TCC (Figure 1A) was found to form both a 1:1 complex and a 2:1 complex, $[2TCC + DMP - H]^-$, which is not included in the calculated complexation ratio. Additionally, a prominent deprotonated homodimer, $[2TCC - H]^-$ was observed, as well as an unidentified ion (*m*/*z* 706), which is also present in the ESI spectrum of TCC alone (Figure S17). For all reagents, appreciable complexation to background chloride ions was also found, with PBP and DIP forming a 1:1 reagent:Cl^- complex and TCC forming a 2:1 complex, $[2TCC + Cl^-]^-$.

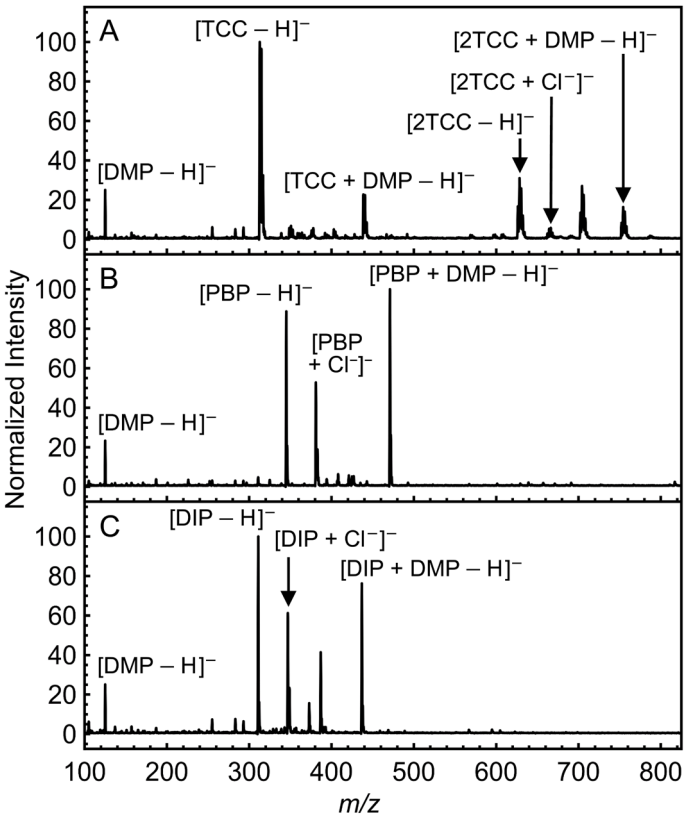

Figure 1. ESI mass spectrum of 30 μM TCC (A), PBP (B), and DIP (C) with 10 μM DMP in 80/20 H_2O/MeOH (v/v%).

For all reagents, the bound:unbound ratio with DMP is nearly an order of magnitude larger than that of all other target molecules studied, with values of 2:1, 5:1 and 4:1 for TCC, PBP, and DIP, respectively (Figure 2A). In addition to minimal steric constraints, the substantial intensity of the complexed species may arise from enhanced surface activity during the electrospray process. As observed for complexation of 18C6 to cationic residues,[11] complexation of reagents with DMP creates a more hydrophobic complex as compared to the free anionic DMP, lowering the free energy of solvation and promoting preferential ionization of the complexed species in ESI.[3] This effect is less pronounced for larger target molecules, where the change in free energy of solvation of the charge site is a smaller fraction of the molecular free energy of solvation.

As compared to DIP and PBP, TCC complexation is significantly lower, which may be partially explained by the propensity of TCC to form both deprotonated and chloride-bound dimers rather than complex with the target molecule. As noted previously for PBP and DIP,[26] one disadvantage of the examined microsolvation reagents is the abundance of the anionic species, $[TCC - H]^-$, $[PBP - H]^-$, and $[DIP - H]^-$. Ideally, the singly deprotonated forms of the complexation reagents would not be as prevalent, as these species may lead to ionization suppression of phosphate species.

3.2 Phosphopeptide Complexation to DIP, PBP and TCC

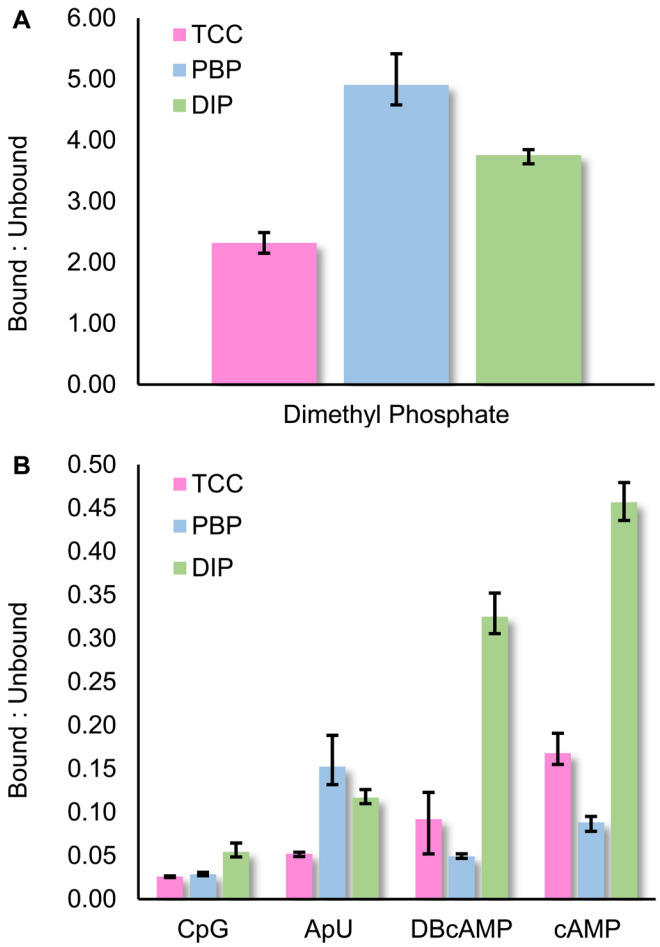

Figure 2. Ratio of bound phosphate + microsolvation reagent complex to unbound phosphate intensities for 30 μM TCC (pink), PBP (blue), or DIP (green) with (A) 10 μM dimethyl phosphate or (B) 10 μM of phosphate-containing biomolecules. Error bars represent the maximum and minimum bound:unbound ratios from three trials.

A variety of small model biomolecules, including RNA dinucleotides, CpG and ApU, and cyclic nucleotides, cAMP and DBcAMP, were chosen to assess the influence of molecular structure on complexation propensity (see Scheme 2 for molecular structures). The bound:unbound complexation ratios for these species are illustrated in Figure 2B. PBP exhibits relatively poor performance for this class of molecules, with complexation ratios ranging from 1:20 for CpG and DBcAMP to 1:10 for cAMP. The most appreciable complexation is observed to ApU, with a complexation ratio exceeding 1:10. Given the strong complexation of PBP to DMP, the substantially decreased affinity for more sterically encumbered species may be explained by steric hindrance arising from the phenyl moieties, consistent with results from electronic structure methods (see section 3.4). Overall, the performance of PBP in binding phosphate moieties is similar to that previously reported for carboxylates,[26] with decreased binding affinity for larger molecules.

TCC performs rather poorly for both ApU and CpG, with ratios of bound:unbound at or below 1:20. In the case of complexation to ApU, the ratio reported is possibly exaggerated, as background ions with the same *m*/*z* as the complex, $[TCC + ApU - H]^-$ (*m*/*z* 885), were observed in samples containing only TCC . However, complexation is improved for the cyclic nucleotides, with complexation ratios of 1:10 and nearly 1:5 for DBcAMP and cAMP, respectively.

Of the three reagents studied, DIP showed the highest binding to the cyclic peptides DBcAMP and cAMP, with bound:unbound ratios of approximately 1:3 and 1:2, respectively. Complexation to CpG was only moderately stronger than that of PBP or TCC. For ApU, DIP performs slightly worse than PBP. Although adduction is observed for DIP, it is notable that the binding to these phosphate species is nearly an order of magnitude less than the complexation previously reported with carboxylate moieties.[26] This result may arise in part from the central location of the phosphate groups as compared to the terminal carboxylate groups, leading to greater steric hindrance. The strong binding of DIP to DMP, where steric effects are minimal, supports this assertion.

3.3 Multisite Complexation to DRVpYIHPF

For larger peptide and protein systems with defined higher-order structures in solution, it is desirable to have concurrent complexation to multiple solvent-accessible sites, which facilitates structural retention upon transfer to vacuum and provides additional tools to study the influence of charge solvation on conformation. We previously reported simultaneous binding of DIP molecules to two anionic carboxylate moieties of the hexapeptide EYMPYE and to the carboxylate and phosphate groups of phosphoserine and phosphotyrosine.[26] Herein, we extend upon these results by examining complexation to DRVpYIHPF, an analog of angiotensin II with a phosphorylated tyrosine residue. Although DRVpYIHPF does not have a well-defined solution-phase structure, it is used in this work to determine if multisite complexation occurs when both phosphate and carboxylate sites are present. There are three possible anionic sites on this peptide: the phosphorylated tyrosine side chain, the aspartic acid side chain, and the C-terminal carboxylic acid. When using TCC, no complexation with the target peptide is observed (Figure S23). Notably, binding may be suppressed by competitive complexation of TCC with trifluoroacetate ($[TFA - H]^-$) in the sample, which yields the complex $[TCC + TFA - H]^-$ as the base peak in the mass spectrum. A similar spectrum is observed when using PBP (Figure 3A), with $[PBP + TFA - H]^-$ as the base peak and minimal complexation with DRVpYIHPF observed, yielding a bound:unbound ratio of 1:10 for the doubly deprotonated, singly bound complex. In addition to adduction with TFA, significant complexation to background chloride anions is observed for PBP, although little to no chloride complexation is observed for TCC.

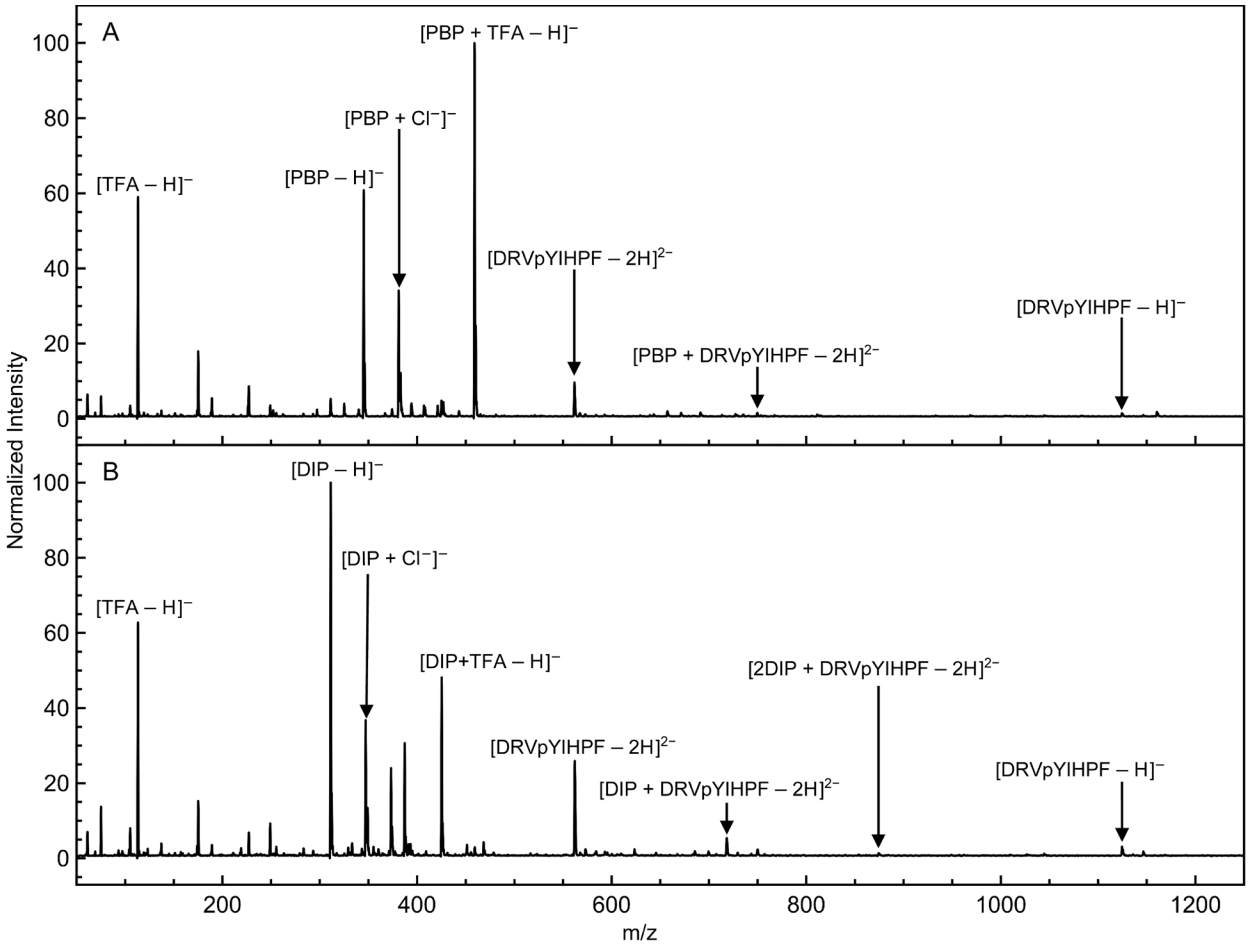

Figure 3. Mass Spectra of 90 μM PBP (A) or DIP (B) and 10 μM DRVpYIHPF in 80/20 H_2O/MeOH (v/v%).

For DIP, the doubly deprotonated, singly bound complex with DRVpYIHPF is present at a bound:unbound ratio of 1:5 as compared to the doubly deprotonated DRVpYIHPF anion (Figure 3B). The doubly bound complex, $[2DIP + DRVpYIHPF - 2H]^{2-}$, is also present at low intensity. It is unclear if this adduction occurs at two carboxylates or at one phosphate and one carboxylate residue. Although pKa values would suggest that deprotonation is more probable at the phosphate moieties than at the carboxylate sites in solution,[50, 51] it is unclear which would preferentially deprotonate in the gas phase. However, the proximity of the two possible carboxylate sites would likely disfavor binding to only these groups. Overall, there is a possibility of simultaneous multisite complexation for DIP, albeit at low intensity, and additional work is required to deduce whether preferential binding occurs at carboxylate or phosphate moieties when multiple charge sites are present.

3.4 DMP Complexes from Electronic Structure Methods

To assess the structural motifs associated with reagent complexation to phosphate moieties, the binding geometry of PBP, TCC, and DIP with DMP was assessed using electronic structure methods. Conformer sampling was performed within a 6 kcal mol^{-1} energy window using the semi-empirical GFN2 method from the CREST software package, yielding 144, 152 and 1277 unique complexation motifs for PBP, TCC, and DIP, respectively. The conformers identified were then optimized at the B3LYP(D3BJ)/def2-TVZP level of theory. After this optimization, the energy spread of predicted conformers for DMP with PBP, TCC, and DIP were 7.0, 6.6 and 9.2 kcal mol^{-1}, respectively. Additionally,

the lowest-energy complexes were reoptimized at the RI-MP2/def2-TVZP level of theory. The computed low-energy structures were consistent independent of the level of theory used (Figure S24). As compared to TCC and PBP, the near tenfold increase of DIP complexes identified by CREST, with 1277 complexes within an energy window of 6 kcal mol^{-1}, is likely explained by the increased flexibility of the DIP backbone.

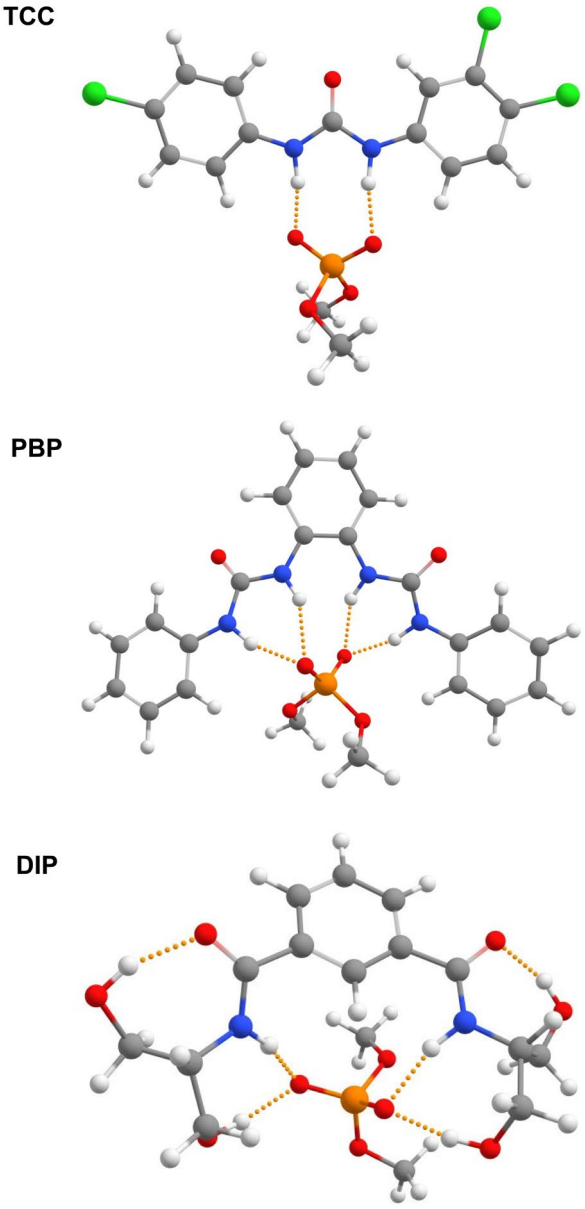

Figure 4. Computed complexation motifs of TCC (top), PBP (center) and DIP (bottom) with DMP. Structures were optimized at the B3LYP(D3BJ)/def2-TZVP level of theory.

Figures 4 and S24 show the lowest-energy structures obtained from the B3LYP and RI-MP2 methods, respectively. For complexation of DIP to DMP, calculations predict four ionic hydrogen bonds, two from the DIP hydroxyl groups and two from the amide hydrogen atoms, all coordinated to the phosphate oxygen atoms. Consistent with previously reported results for binding to carboxylate moieties,[26] the phosphate group is not fully coordinated with all potential hydrogen bond donors of DIP,

with two of the hydroxyl groups instead forming intramolecular hydrogen bonds. Notably, the methyl groups of DMP extend beneath the binding pocket and away from DIP, minimizing steric hindrance. The ten lowest-energy conformers exhibited a wide range of orientations for the DIP hydroxyl groups and the DMP within the binding pocket (see Figure S25). The energy difference between these conformers was also relatively small, with all ten structures yielding an electronic energy within 1 kcal mol^{-1} of the lowest-energy conformer (Table S1). These results suggest that complexation may exhibit a degree of entropic favorability, although this conformational freedom is likely present for the uncomplexed reagent as well. Indeed, in solution the complexation of DIP with carboxylates is not favorable, likely reflecting an entropic penalty to binding.[26] However, the complexation in vacuum is strongly favored enthalpically in the absence of steric constraints, as reflected in the high complexation ratios for DIP with DMP.

For complexation of PBP with DMP, four ionic hydrogen bonds are also observed, all arising from the amide hydrogen atoms of the urea groups coordinated with the phosphate oxygen atoms. The complexation motif is pseudo-symmetric, with two hydrogen bonds coordinating each of the urea moieties to an oxygen atom of DMP. Within the 144 conformers identified, there is a slight variation in the torsional angle of the phenyl groups that facilitates complexation. However, most of the conformational space sampled corresponds to the rotation and translation of the DMP anion within the binding pocket. In contrast to DIP, the ten lowest-energy conformers for PBP with DMP (Figure S26) exhibit nearly identical orientation of PBP. However, the relative energy of these conformers is much broader (ca. 5 kcal mol^{-1}, Table S1), reflecting the large steric penalty for reorientation of DMP within the binding pocket. Thus, the proximity of the bulky phenyl groups to the anion binding site suggests that complexation to larger molecules containing a phosphate group will be hindered, consistent with experimental results.

Of the three complexation reagents studied, TCC shows the least defined binding pocket, as only two ionic hydrogen bonds are predicted between the amide hydrogens of TCC and the phosphate oxygen atoms of DMP. Similar to PBP, the 152 conformers sampled indicate a variety of DMP orientations in binding to TCC, with minimal alterations to the rigid backbone of TCC. This result is again observable in the conformations of the ten lowest-energy structures (Figure S27), which all exhibit similar orientations of TCC. Because the DMP methyl groups protrude above and below the plane of complexation, little evidence for steric hindrance of complexation is observed, and the relative energies of the lowest-energy conformers are quite similar as a result (<1.5 kcal mol^{-1}, Table S1). However, this low energy spread depends strongly on the orientation of any groups extending from the phosphate group, and possible conformations may be restricted in larger molecules. The reduced size of the hydrogen bonding network, as compared to PBP and DIP, may explain the decreased complexation propensity observed for TCC, despite the relatively strong binding affinity observed for TCC in organic solvent.[28]

4. Conclusion

Of the three reagents examined for complexation with phosphate moieties, DIP is found to exhibit the best performance, forming complexes with both terminal and central phosphate groups. These results indicate that DIP can be used as a suitable gas-phase microsolvation reagent for the preservation of solution-phase structure and the study of charge microsolvation effects. As compared to PBP, DIP shows slightly lower complexation for DMP as well as ApU. However, DIP shows more favorable complexation to the cyclic nucleotides (DBcAMP and cAMP) and exhibits multisite adduction in DRVpYIHPF, albeit at low intensities. Further improvements in binding affinity are desirable to improve multisite adduction in larger systems. The limited complexation of PBP to larger phosphates may be explained by the bulky phenyl groups flanking the binding pocket, which suggests that steric hindrance strongly influences the complexation propensity of charge recognition reagents with larger biomolecules. TCC showed moderate complexation to most systems studied. From the target molecules studied in this work, complexation affinity is associated with the accessibility of the binding site, as determined by steric constraints, as well as the strength of the hydrogen bond network formed. A decrease in the free energy of solvation upon

complex formation may also yield enhanced signal of the complexed species, especially for smaller molecules.

Future work will focus on the examination of structural retention upon complexation to DIP. To this point, we have demonstrated the possibility of complex formation at anionic sites in biomolecules, but further spectroscopic characterization is required to determine if solution-phase structure is retained upon complexation. Additionally, further analysis is required to assess the influence of DIP complexation on low-energy gas-phase conformation. In summary, DIP is a suitable reagent for gas-phase complexation both carboxylate and phosphate sites in biomolecules, presenting a sterically accessible binding pocket supported by an extended hydrogen bonding network. This complexation is promising for the potential of solution-phase structure retention and microsolvation studies.

5. CRediT Statement

Madeline Schultz: Conceptualization, Methodology, Formal analysis, Writing - Original Draft. **Neil A. Ellis:** Investigation, Formal analysis, Writing - Original Draft. **Nwanne D. Banor:** Software. **Daniel A. Thomas:** Supervision, Funding acquisition, Conceptualization, Writing - Review & Editing.

6. Acknowledgements

This work was supported by NSF grant CHE-2212926. NAE was supported by a summer research fellowship from the College of Arts and Sciences at the University of Rhode Island. NDB was supported by a Presidential Fellowship through the Graduate School at the University of Rhode Island. Computational resources were provided by the URI Center for Computational Research.

7. References

(1) Nagornova, N. S.; Rizzo, T. R.; Boyarkin, O. V. Interplay of Intra- and Intermolecular H-Bonding in a Progressively Solvated Macrocyclic Peptide. *Science* **2012**, *336* (6079), 320-323. DOI: https://doi.org/10.1126/science.1218709.
(2) Steinberg, M. Z.; Breuker, K.; Elber, R.; Gerber, R. B. The dynamics of water evaporation from partially solvated cytochrome c in the gas phase. *Phys. Chem. Chem. Phys.* **2007**, *9* (33), 4690-4697. DOI: https://doi.org/10.1039/B705905A.
(3) Kebarle, P.; Verkerk, U. H. Electrospray: From ions in solution to ions in the gas phase, what we know now. *Mass Spectrom. Rev.* **2009**, *28* (6), 898-917. DOI: https://doi.org/10.1002/mas.20247.
(4) Fenn, J. B.; Mann, M.; Meng, C. K.; Wong, S. F.; Whitehouse, C. M. Electrospray Ionization for Mass Spectrometry of Large Biomolecules. *Science* **1989**, *246* (4926), 64-71. DOI: https://www.doi.org/10.1126/science.2675315.
(5) Konermann, L.; Ahadi, E.; D. Rodriguez, A.; Vahidi, S. Unraveling the Mechanism of Electrospray Ionization. *Anal. Chem.* **2012**, *85* (1), 2-9. DOI: https://doi.org/10.1021/ac302789.
(6) Warnke, S.; von Helden, G.; Pagel, K. Protein Structure in the Gas Phase: The Influence of Side-Chain Microsolvation. *J. Am. Chem. Soc.* **2013**, *135* (4), 1177-1180. DOI: https://doi.org/10.1021/ja308528d.
(7) Baldauf, C.; Rossi, M. Going clean: Structure and dynamics of peptides in the gas phase and paths to solvation. *J. Phys. Condens. Matter* **2015**, *27* (49). DOI: http://doi.org/10.1088/0953-8984/27/49/493002.
(8) Breuker, K.; McLafferty, F. W. Stepwise evolution of protein native structure with electrospray into the gas phase, 10−12 to 102 s. *Proc. Natl. Acad. Sci.* **2008**, *105* (47), 18145-18152.
(9) Bonner, J. G.; Hendricks, N. G.; Julian, R. R. Structural Effects of Solvation by 18-Crown-6 on Gaseous Peptides and TrpCage after Electrospray Ionization. *J. Am. Soc. Mass Spectrom.* **2016**, *27* (10), 1661-1669.
(10) Silzel, J. W.; Murphree, T. A.; Paranji, R. K.; Guttman, M. M.; Julian, R. R. Probing the Stability of Proline Cis/Trans Isomers in the Gas Phase with Ultraviolet Photodissociation. *Journal of the American Society for Mass Spectrometry* **2020**, *31* (9), 1974-1980. DOI: https://doi.org/10.1021/jasms.0c00242.
(11) Julian, R. R.; Beauchamp, J. L. Site specific sequestering and stabilization of charge in peptides by supramolecular adduct formation with 18-crown-6 ether by way of electrospray ionization. *Int J. Mass Spectrom.* **2001**, *210-211*, 613-623. DOI: https://doi.org/10.1016/S1387-3806(01)00431-6.
(12) McNary, C. P.; Nei, Y. W.; Maitre, P.; Rodgers, M. T.; Armentrout, P. B. Infrared multiple photon dissociation action spectroscopy of protonated glycine, histidine, lysine, and arginine complexed with 18-crown-6 ether. *Phys. Chem. Chem. Phys.* **2019**, *21* (23), 12625-12639. DOI: https://doi.org/10.1039/C9CP02265A.

(13) Liu, Z.; Cheng, S.; R. Gallie, D.; R. Julian, R. Exploring the Mechanism of Selective Noncovalent Adduct Protein Probing Mass Spectrometry Utilizing Site-Directed Mutagenesis To Examine Ubiquitin. *Anal. Chem.* **2008**, *80* (10), 3846-3852. DOI: https://doi.org/10.1021/ac800176u.
(14) González Flórez, A. I.; Ahn, D.-S.; Gewinner, S.; Schöllkopf, W.; von Helden, G. IR spectroscopy of protonated leu-enkephalin and its 18-crown-6 complex embedded in helium droplets. *Phys. Chem. Chem. Phys.* **2015**, *17* (34), 21902-21911. DOI: http://doi.org/10.1039/C5CP02172C.
(15) Chen, Y.; Rodgers, M. T. Structural and Energetic Effects in the Molecular Recognition of Protonated Peptidomimetic Bases by 18-Crown-6. *J. Am. Chem. Soc.* **2012**, *134* (4), 2313-2324. DOI: https://doi.org/10.1021/ja2102345.
(16) Ko, J. Y.; Heo, S. W.; Lee, J. H.; Oh, H. B.; Kim, H.; Kim, H. I. Host-guest chemistry in the gas phase: complex formation with 18-crown-6 enhances helicity of alanine-based peptides. *J. Phys. Chem. A* **2011**, *115* (49), 14215-14220. DOI: https://doi.org/10.1021/jp208045a.
(17) Oh, Y.-H.; Oh, H. B.; Lee, S. Structural connectivity of 18-Crown-6/H+/L-tryptophan noncovalent complexes in gas phase and in solution: Delineating host–guest–solvent interactions in solution from gas phase structures. *Inter. J. Quantum Chem.* **2024**, *124* (1), e27337. DOI: https://doi.org/10.1002/qua.27337.
(18) Ly, T.; Julian, R. R. Using ESI-MS to Probe Protein Structure by Site-Specific Noncovalent Attachment of 18-Crown-6. *J. Am. Soc. Mass Spectrom.* **2006**, *17* (9), 1209-1215. DOI: https://doi.org/10.1016/j.jasms.2006.05.007.
(19) Tao, Y.; Julian, R. R. Investigation of peptide microsolvation in the gas phase by radical directed dissociation mass spectrometry. *Int. J. Mass Spectrom.* **2016**, *409*, 81-86. DOI: http://doi.org/10.1016/j.ijms.2016.10.001.
(20) Tao, Y.; Julian, R. R. Factors that influence competitive intermolecular solvation of protonated groups in peptides and proteins in the gas phase. *J. Am. Soc. Mass Spectrom.* **2013**, *24* (11), 1634-1640. DOI: https://doi.org/10.1007/s13361-013-0684-z.
(21) Stedwell, C. N.; Galindo, J. F.; Gulyuz, K.; Roitberg, A. E.; Polfer, N. C. Crown complexation of protonated amino acids: Influence on IRMPD spectra. *J. Phys. Chem. A* **2013**, *117* (6), 1181-1188. DOI: https://doi.org/10.1021/jp305263b.
(22) Ly, T.; Julian, R. R. Protein-metal interactions of calmodulin and α-synuclein monitored by selective noncovalent adduct protein probing mass spectrometry. *J. Am. Soc. Mass Spectrom.* **2008**, *19* (11), 1663-1672. DOI: https://doi.org/10.1016/j.jasms.2008.07.006.
(23) Zhou, L.; Liu, Z.; Guo, Y.; Liu, S.; Zhao, H.; Zhao, S.; Xiao, C.; Feng, S.; Yang, X.; Wang, F. Ultraviolet Photodissociation Reveals the Molecular Mechanism of Crown Ether Microsolvation Effect on the Gas-Phase Native-like Protein Structure. *J. Amer. Chem. Soc.* **2023**, *145* (2), 1285-1291. DOI: https://doi.org/10.1021/jacs.2c11210.
(24) Moore, B. N.; Hamdy, O.; Julian, R. R. Protein structure evolution in liquid DESI as revealed by selective noncovalent adduct protein probing. *Int. J. Mass Spectrom.* **2012**, *330-332*, 220-225. DOI: https://doi.org/10.1016/j.ijms.2012.08.013.
(25) Bruce, M. I.; Zwar, J. A. Cytokinin activity of some substituted ureas and thioureas. *Proc. R. Soc. B* **1966**, *165* (999), 245-265. DOI: https://doi.org/10.1098/rspb.1966.0067.
(26) Schultz, M.; Parker, S. L.; Fernando, M. T.; Wellalage, M. M.; Thomas, D. A. Diserinol Isophthalamide: A Novel Reagent for Complexation with Biomolecular Anions in Electrospray Ionization Mass Spectrometry. *J. Amer. Soc. Mass Spectrom.* **2023**, *34* (4), 745-753. DOI: https://doi.org/10.1021/jasms.3c00010.
(27) Iacopetta, D.; Catalano, A.; Ceramella, J.; Saturnino, C.; Salvagno, L.; Ielo, I.; Drommi, D.; Scali, E.; Plutino, M. R.; Rosace, G.; et al. The Different Facets of Triclocarban: A Review. *Molecules* **2021**, *26* (9). DOI: https://doi.org/10.3390/molecules26092811.
(28) Rüütel, A.; Tshepelevitsh, S.; Leito, I. One Hundred Carboxylate Receptors. *J. Org. Chem.* **2022**, *87*, 14186-14193. DOI: https://doi.org/10.1021/acs.joc.2c01725.
(29) Yue, Y.; Wang, Z.; Zhang, Y.; Wang, Z.; Lv, Q.; Liu, J. Binding of triclosan and triclocarban to pepsin: DFT, spectroscopic and dynamic simulation studies. *Chemosphere* **2019**, *214*, 278-287. DOI: https://doi.org/10.1016/j.chemosphere.2018.09.108.
(30) Barišić, D.; Lešić, F.; Tireli Vlašić, M.; Užarević, K.; Bregović, N.; Tomišić, V. Anion binding by receptors containing NH donating groups – What do anions prefer? *Tetrahedron* **2022**, *120*, 132875. DOI: https://doi.org/10.1016/j.tet.2022.132875.
(31) Grimme, S. Exploration of Chemical Compound, Conformer, and Reaction Space with Meta-Dynamics Simulations Based on Tight-Binding Quantum Chemical Calculations. *J. Chem. Theory Comput.* **2019**, *15* (5), 2847-2862. DOI: https://doi.org/10.1021/acs.jctc.9b00143.
(32) Bannwarth, C.; Caldeweyher, E.; Ehlert, S.; Hansen, A.; Pracht, P.; Seibert, J.; Spicher, S.; Grimme, S. Extended tight-binding quantum chemistry methods. *Rev. Comput. Mol. Sci.* **2021**, *11* (2). DOI: https://doi.org/10.1002/wcms.1493.
(33) Pracht, P.; Bohle, F.; Grimme, S. Automated exploration of the low-energy chemical space with fast quantum chemical methods. *Phys. Chem. Chem. Phys.* **2020**, *22* (14), 7169-7192. DOI: https://doi.org/10.1039/C9CP06869D.
(34) Bannwarth, C.; Ehlert, S.; Grimme, S. GFN2-xTB—An Accurate and Broadly Parametrized Self-Consistent Tight-Binding Quantum Chemical Method with Multipole Electrostatics and Density-Dependent Dispersion Contributions. *J. Chem. Theory Comput.* **2019**, *15* (3), 1652-1671. DOI: https://doi.org/10.1021/acs.jctc.8b01176.

(35) Neese, F. The ORCA program system. *WIREs Comput. Mol. Sci.* **2012**, *2* (1), 73-78. DOI: https://doi.org/10.1002/wcms.81.
(36) Neese, F. Software update: The ORCA program system—Version 5.0. *WIREs Computer. Mol. Sci.* **2022**, *12* (5), e1606. DOI: https://doi.org/10.1002/wcms.1606.
(37) Becke, A. D. Density-functional thermochemistry. III. The role of exact exchange. *J. Chem. Phys.* **1993**, *98* (7), 5648. DOI: https://doi.org/10.1063/1.464913.
(38) Lee, C.; Yang, W.; Parr, R. G. Development of the Colle-Salvetti correlation-energy formula into a functional of the electron density. *Phys. Rev. B Condens. Matter* **1988**, *37* (2), 785-789. DOI: https://doi.org/10.1103/PhysRevB.37.785.
(39) Stephens, P. J.; Devlin, F. J.; Chabalowski, C. F.; Frisch, M. J. Ab Initio Calculation of Vibrational Absorption and Circular Dichroism Spectra Using Density Functional Force Fields. *J. Phys. Chem.* **1994**, *98* (45), 11623-11627. DOI: https://doi.org/10.1021/j100096a001.
(40) Grimme, S.; Ehrlich, S.; Goerigk, L. Effect of the damping function in dispersion corrected density functional theory. *J. Comput. Chem.* **2011**, *32* (7), 1456-1465. DOI: https://doi.org/10.1002/jcc.21759.
(41) Grimme, S.; Antony, J.; Ehrlich, S.; Krieg, H. A consistent and accurate ab initio parametrization of density functional dispersion correction (DFT-D) for the 94 elements H-Pu. *J. Chem. Phys.* **2010**, *132* (15), 154104. DOI: https://doi.org/10.1063/1.3382344.
(42) Weigend, F.; Ahlrichs, R. Balanced basis sets of split valence, triple zeta valence and quadruple zeta valence quality for H to Rn: Design and assessment of accuracy. *Phys. Chem. Chem. Phys.* **2005**, *7* (18), 3297-3305. DOI: http://doi.org/10.1039/B508541A.
(43) Petrenko, T.; Kossmann, S.; Neese, F. Efficient time-dependent density functional theory approximations for hybrid density functionals: Analytical gradients and parallelization. *J. Chem. Phys.* **2011**, *134* (5), 054116. DOI: https://doi.org/10.1063/1.3533441.
(44) Weigend, F. Accurate Coulomb-fitting basis sets for H to Rn. *Phys. Chem. Chem. Phys.* **2006**, *8* (9), 1057-1065. DOI: https://doi.org/10.1039/B515623H.
(45) Weigend, F.; Häser, M.; Patzelt, H.; Ahlrichs, R. RI-MP2: optimized auxiliary basis sets and demonstration of efficiency. *Chem. Phys. Lett.* **1998**, *294* (1), 143-152. DOI: https://doi.org/10.1016/S0009-2614(98)00862-8.
(46) Weigend, F.; Häser, M. RI-MP2: first derivatives and global consistency. *Theor. Chem. Acc.* **1997**, *97* (1), 331-340. DOI: https://doi.org/10.1007/s002140050269.
(47) Hellweg, A.; Hättig, C.; Höfener, S.; Klopper, W. Optimized accurate auxiliary basis sets for RI-MP2 and RI-CC2 calculations for the atoms Rb to Rn. *Theor. Chem. Acc.* **2007**, *117* (4), 587-597. DOI: http://doi.org/10.1007/s00214-007-0250-5.
(48) Weigend, F. A fully direct RI-HF algorithm: Implementation, optimised auxiliary basis sets, demonstration of accuracy and efficiency. *Phys. Chem. Chem. Phys.* **2002**, *4* (18), 4285-4291. DOI: https://doi.org/10.1039/B204199P.
(49) Oss, M.; Kruve, A.; Herodes, K.; Leito, I. Electrospray Ionization Efficiency Scale of Organic Compounds. *Anal. Chem.* **2010**, *82* (7), 2865-2872. DOI: https://doi.org/10.1021/ac902856t.
(50) Wojciechowski, M.; Grycuk, T.; Antosiewicz, J. M.; Lesyng, B. Prediction of Secondary Ionization of the Phosphate Group in Phosphotyrosine Peptides. *Biophys. J.* **2003**, *84* (2), 750-756. DOI: https://doi.org/10.1016/S0006-3495(03)74894-2.
(51) Grimsley, G. R.; Scholtz, J. M.; Pace, C. N. A summary of the measured pK values of the ionizable groups in folded proteins. *Prot. Sci.* **2009**, *18* (1), 247-251. DOI: https://doi.org/10.1002/pro.19.